The Performance and Durability of single-layer Sol-gel Anti-reflection Coatings

Gerald Womack[a], Kenan Isbilir[a], Fabiana Lisco[a], Geraldine Durand[b,c], Alan Taylor[b], and John M Walls[a]

[a]CREST (Centre for Renewable Energy Systems and Technology), The Wolfson School of Mechanical, Electrical and Manufacturing Engineering, Loughborough University, Loughborough, LE11 3TU, United Kingdom

[b]TWI Ltd, Granta Park, Great Abington, Cambridge, CB21 6AL, United Kingdom

[c] London South Bank University, 103 Borough Road, London SE1 0AA, United Kingdom

Corresponding author: Dr. G. Womack. Email: g.womack@lboro.ac.uk

Additional contacts: Mr. K. Isbilir, K.Isbilir@lboro.ac.uk, Dr. F. Lisco, F.Lisco@lboro.ac.uk, Prof. J. M. Walls, J.M.Walls@lboro.ac.uk.: Prof. A. Taylor, alan.taylor@twi.co.uk, Prof. Geraldine Durand, durandg@lsbu.ac.uk

Abstract

A significant source of energy loss in photovoltaic (PV) modules is caused by reflection from the front cover glass surface. Reflection from the cover glass causes a loss of ~4% at the air-glass interface. Only a single air-glass interface occurs on crystalline silicon solar modules as they have an EVA layer between the cover glass and the silicon absorber. EVA is index matched to glass, therefore eliminating a second air-glass interface. A single-layer anti-reflection coating (ARC) on the outer surface of the cover glass is effective at reducing reflection losses over the wavelength range of most PV devices. The coating investigated in this work reduces the reflectance loss at the glass surface by 74%. However, the long-term durability of sol-gel coatings has not been established. In this work, we investigate the damage resistance of a single-layer closed-surface hard coat ARC, deposited using sol-gel methods by applying a variety of accelerated weathering, scratch and abrasion test methods.

The reflectance of a commercially available sol-gel ARC was measured and then the coating was put through a series of durability and environmental tests. The coating appears resistant to damage from heating and can withstand temperatures higher than the phase change temperature of soda-lime glass. Scratch testing demonstrated that the sol-gel AR is relatively hard and difficult to remove from the substrate surface. Pull tests and cross-hatch testing also

confirmed the strong adhesion of the coating. Weathering experiments show some degradation in weighted average reflectance, particularly an increase in reflectance of 0.6-0.9% after 1000 hours of exposure to damp heat. Testing also showed a vulnerability to acid attack.

The commercial ARC had a low water contact angle, which means the coatings are hydrophilic and, therefore, hygroscopic and susceptible to water damage over extended periods of time.

Keywords: Anti-reflection, coating, solution-gelation, hard coat, dip-coated.

1 Introduction

Single-layer anti-reflection coatings (ARCs) are currently used to reduce reflection losses from the surface of the cover glass of crystalline silicon photovoltaic (PV) modules. They are also applied to cover glass on substrate configuration thin film modules such as CIGS, and directly to the glass superstrate for thin film cadmium telluride (CdTe). Mainstream technology solar panels are provided with a 25 year warranty, so ARCs for solar modules must be durable on a time-scale matching this industry standard. Solar modules undergo a series of accelerated environmental and durability standard tests to ensure they can withstand decades of outdoor exposure, in accordance with the International Electrotechnical commission (IEC) standards (IEC 2016). As ARCs will undergo the same stresses and weathering as the solar panel it is applied to, IEC module standards should also be applied to ARCs designed for application on solar modules. Coatings on cover glass are continuously exposed to the environment, and additional testing protocols must ensure that all possible mechanisms resulting in degradation are simulated by the testing protocols.

There are different types of ARC available. The choice of coating is governed by considerations of performance, durability, ease of application, and cost. At present, the industry is predominantly using low-cost single-layer sol-gel coatings, which are deposited in atmospheric conditions using solution processing techniques. These coatings provide effective anti-reflection properties and are often presented with some assurance of the longevity of the coating, such as no visual degradation after 1000 hours of damp heat exposure and resistance to 60 hours of exposure to sulfuric and nitric acid (Guo et al. 2017; Wang & Shen 2010).

Sol-gel ARCs use many possible precursor materials, such as: silica, metal alkoxides, and alumina (Fabes et al. 1993; Mammeri et al. 2005; Guo et al. 2006; Wang & Xiong 2014). Sol-gel processing offers the advantages of high manufacturing rates, mass production and low production costs. Sol-gel can have a variety of simultaneous functions (Pagliaro et al. 2009; Schottner 2001; Han et al. 2007; Sanchez et al. 2011; Çamurlu et al. 2012; Tao et al. 2016). One method of achieving a multifunction coating is by depositing different sol-gel layers on top of one another. For example, a hydrophobic coating can be deposited on top of an anti-reflection coating to produce a dual function coating. However, considering the curing times and temperatures involved in sol-gel deposition, and the requirement for pre-coated glass in PV manufacturing, the stacking of different sol-gel coatings becomes less desirable due to manufacturing costs and complexity. Alternatively, the ARC can be produced with a deliberately rough surface on the nanoscale to achieve a hydrophobic effect. However, the roughness and porosity of such coatings results in a trade-off with coating transmission (Xu et al. 2017). It has been noted that air bubbles trapped within rough coatings have an important role in achieving hydrophobicity in rough sol-gel ARCs (Wang & Xiong 2014). Hydrophobicity has been achieved through a variety of novel chemical functionalisation and deposition techniques (Xu et al. 2017).

Porous sol-gel coatings are known to be mechanically fragile and vulnerable to water ingress and contamination, which affects the refractive index and, therefore, the transmissivity and reflectivity of the ARC (Cooper & Cox 1996; Vilarigues & da Silva 2006). It is possible to improve the vulnerability to water damage of sol-gel coatings. However, there is a trade-off between the optical properties of the coating, hydrophobicity, and resistance to mechanical damage. Commercial sol-gel ARCs are hydrophilic hard coatings with a non-porous closed top surface, which are more resistant to water damage than traditional porous silica coatings but are still affected. Sol-gel hard coatings have shown increased resistance to damp heat exposure, when compared to porous sol-gel ARCs (Guo et al. 2017). In this work, we report on the results of extensive tests to evaluate the performance and durability of a commercially sourced closed surface sol-gel hard coat.

A variety of assessment tests should be performed to test the durability of sol-gel anti-reflective surface coatings (Vicente et al. 2008). The scratch resistance of the ARC was measured using micro-indentation scratch tests (Chen et al. 2011). Pull test and crosshatch tests have also been used to evaluate the adhesion of the coating on the substrate surface. In the case of solar cell technologies with a superstrate configuration, it is attractive for an ARC

to be on the surface of the glass before the cell is deposited on the other side, simplifying the manufacturing process. This necessitates resistance to the high temperatures (up to 500°C) involved in the thin film photovoltaic stack deposition (Womack et al. 2015). By performing standard tests in damp heat (Osterwald & McMahon 2008), temperature cycling (Osterwald & McMahon 2008), and acid attack (ISO 2012), resistance to weathering damage has been assessed. The water contact angle of the coatings has also been measured, giving insight into the hydrophobicity/hydrophilicity of the coating. New multi-variate analysis methods are being developed to enable an effective and meaningful comparison between different coatings and surface treatment methods (Wojdyła et al. 2017). A coating is considered durable and fit for purpose once it has passed all tests.

For comparison, high performance multilayer broadband ARCs (MAR), deposited using high vacuum PVD techniques, are an alternative to sol-gel coatings (Kaminski et al. 2014). The results of applying this battery of environmental and durability tests to MARs has been reported (Womack et al. 2017).

2 Sol-gel single-layer coating design

2.1 Single-layer anti-reflection

The mathematics governing the ideal refractive index of a coating for maximum transmission was first derived by Lord Rayleigh (A. E. Conrady 1929). The refractive index of an optimised single-layer ARC, with clearly defined step changes in refractive index, is the square root of the refractive index of the exit medium multiplied by the square root of the refractive index of the entry medium or expressed mathematically:

$$n_c = \sqrt{n_1 n_2} \tag{1}$$

Where n_c is the refractive index of the coating, n_1 is the refractive index of the entrance medium, and n_2 is the refractive index of the exit medium. In the case of an air-glass interface, assuming the refractive index of glass is ~1.5, the ideal refractive index for a single-layer ARC is ~1.22. By manipulating the ratio between silica and voids within a coating, a refractive index as low as 1.22 is achievable through sol-gel deposition.

Single-layer anti-reflection is also achieved through the manipulation of reflections from different layer interfaces to create destructive interference, between the glass-coating interface and the coating-air interface. As shown in Figure 1, the ideal thickness of

interference based single-layer coatings is a quarter the wavelength of incident light. As the thickness of a coating can only be a quarter length of a single wavelength, the effectiveness of single-layer ARC is greatest at a single wavelength. Additionally, as the path length through the single-layer ARC depends on the path taken through the coating, destructive interference is most effective at a single angle of incidence.

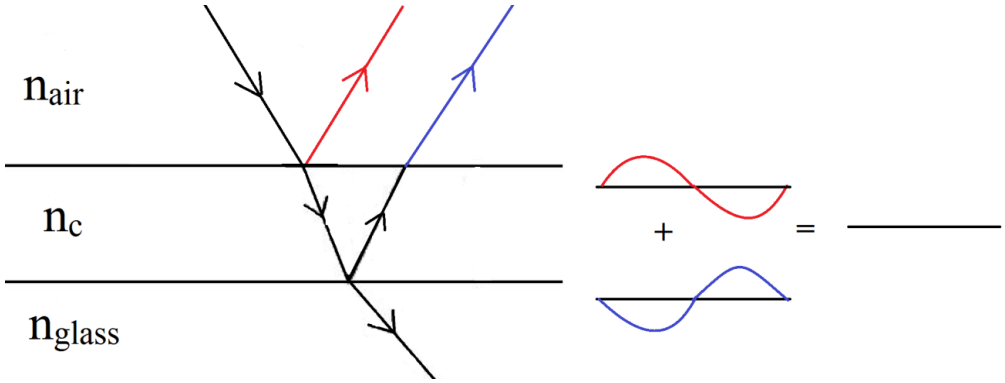

Figure 1: The anti-reflection effect of a single-layer ARC, reflected light from two interfaces cause destructive interference.

2.2 Chemistry and deposition method

Although magnesium fluoride has a lower refractive index than SiO_2 (~1.38 for MgF_2 and ~1.46 for SiO_2), SiO_2 is readily available and abundant. Silica (SiO_2) is the most common material used in single-layer AR coatings deposited through the sol-gel method. SiO_2 has a low refractive index (n=1.45-1.47 at 550nm). The refractive index of a material lowers as the void percentage (air pockets within the film) increases. As the porosity of the coating increases, the friability of the coating increases. The refractive index of deposited coatings have been reported to be as low as 1.15 (Cai et al. 2014).

It is possible to control the parameters of sol-gel deposition, such as dip speed, solution viscosity, and spin rates to grant greater control over the dimensions of microstructures in sol-gel surfaces, such as surface area and thickness, void radius, and volume (Brinker & Scherer 1990; Deubener et al. 2009). Thickness control in sol-gel deposition is fairly good (Faustini et al. 2010). The refractive index of the sol-gel coatings tested in this work was measured by spectroscopic ellipsometry to be ~1.26.

Most sol-gel materials used for ARC coatings use alkoxysilanes as the precursors, to grow silica particulates (Stöber Spheres) or to bind together pre-existing silica particulates. A range of alkoxysilanes have been used, including high silica content systems (Meredith & Harvey

2006). Some patents also describe use of the commercially available colloidal silica, or use hollow ceramic spheres(Thies et al. 2011; Buskens et al. 2016).

The coating investigated in this work was a procured commercially. This coating is broadly based on the technology described by Thies (Arfsten et al. 2011). However, the exact deposition method and chemistry of the coating is not known in detail.

3 Sol-Gel anti-reflection optical performance and imaging

The optical performance of single-layer coatings depends on the refractive index and thickness of the coating. To maintain anti-reflective performance for solar modules across wide wavelength ranges, an ARC must have a reflection minimum at the most energy dense region of the solar spectrum. The AM1.5 spectrum is heavily weighted in the 350nm to 650nm wavelength range. Consequently, it is reasonable to use a coating designed for use in the visible light wavelengths across broader wavelength ranges, as long as the coating remains transparent across the broader wavelength range. The ARC investigated in this work does not heavily absorb in the 350nm-1100nm wavelength range, and so can be used with all PV technologies. This means the coating is optically suitable for most solar cell technologies of varying bandgaps, including crystalline silicon and CIGS, with a bandgap of ~1.13eV (350nm-~1100nm), and CdTe with a bandgap of ~1.46eV (350nm-~850nm). Glass begins to absorb light heavily between 350nm-400nm. The performance of the coating was measured for different PV technologies by calculating the weighted average reflectance (WAR) of the coating across different wavelength ranges. The measured reflection from the ARC coated glass compared to uncoated glass is shown in Figure 2.

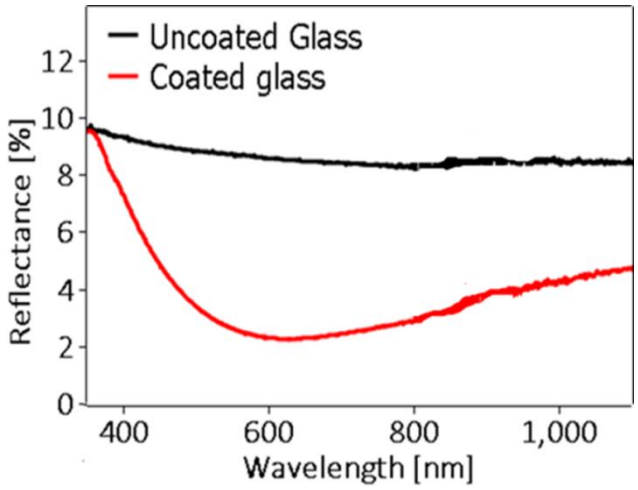

Figure 2: A comparison of the measured reflectances from both back and front surfaces of an uncoated glass sample and an ARC coated sample coated on both sides, between 350nm and 1100nm

The reflectance of the sol-gel ARC was measured using a Varian Cary 5000 UV-vis-IR spectrophotometer. Reflectance from both sides of the glass samples was considered to allow for a fair comparison of the reflectance of the coating to that of uncoated glass, with no manipulation of the data. Across the CdTe wavelength range (350nm, 850nm), the WAR from a 3mm soda-lime glass slide, coated on both sides with sol-gel ARC, is reduced to 2.2% across 2 interfaces, from 8.72% on bare glass. To maintain consistency and avoid manipulation of the data, all results presented in this work consider both interfaces of the samples, as this is consistent throughout the work comparisons of WAR before and after testing is still meaningful. In industry the coating would only be on one side of the glass and the PV cell on the other. Across the CIGS/crystalline silicon wavelength range (350nm, 1100nm) WAR is reduced to 2.7% from 8.62%.

A comparison of the effectiveness of the ARC across different PV technology wavelength ranges is shown in Table 1. The results show that because the AM1.5 solar spectrum is heavily weighted in the visible light region of the electro-magnetic spectrum, extending the wavelength range has a limited effect on the overall optical performance of the coating.

Table 1: A comparison of coating reflectance across the wavelength ranges of different PV technologies.

	Sol-gel ARC WAR [%]	Reflectance percentage reduction sol-gel ARC [%]
CdTe	2.2	74
CIGS/Crystalline Silicon	2.7	69

An SEM image of a cross-section through the ARC on glass is shown in

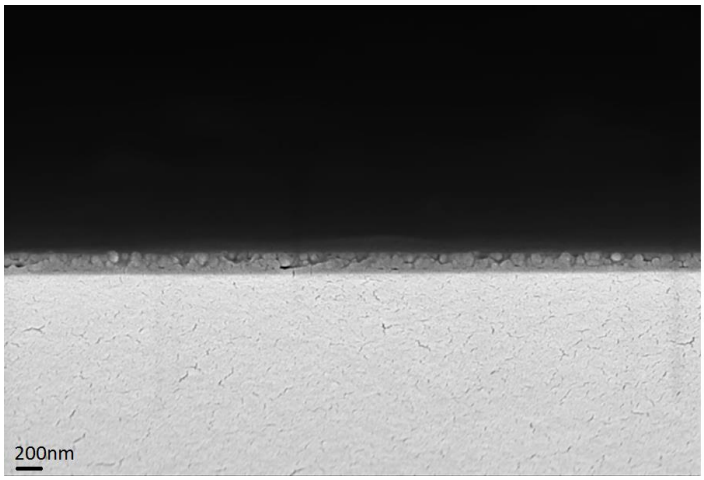

Figure 3. The coating is ~180nm thick with little variation in thickness visible in the image. The surface is mostly closed, but some defects that may make the coating susceptible to water damage are apparent. A close up of a defect is shown in Figure 4.

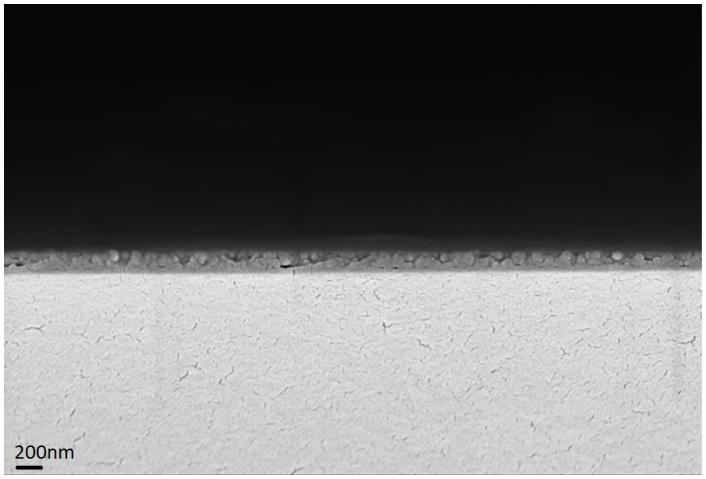

Figure 3: An SEM image of a cross section of the ARC on a soda-lime glass substrate Image courtesy of TWI

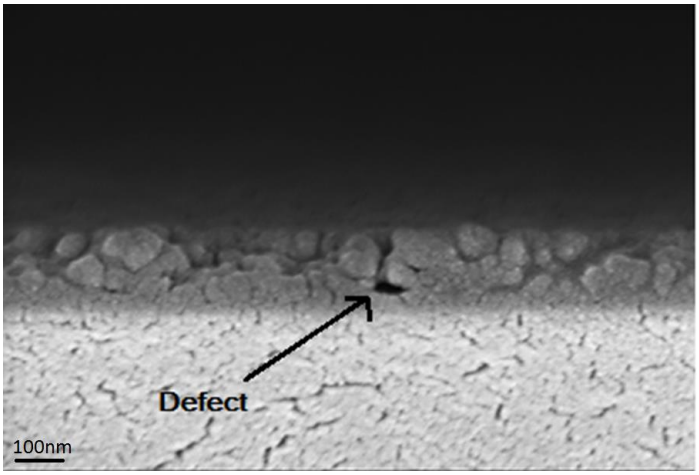

Figure 4: A higher magnification image of an ARC cross section, showing a labelled defect where the coating is open to water damage – Image courtesy of TWI.

4 Durability of the Sol-gel Coatings

4.1 Adhesion

Adhesion is an important measure of coating durability, as low adhesion implies the coating is easy to remove from the substrate surface. Adhesion of the sol-gel coatings was measured using the pull test and the cross hatch test methods.

4.1.1 Pull Test

Pull tests were carried out in accordance with standards ISO 4624 and ASTM D4541(ISO 2002; ASTM 2002). Aluminium dollies were fixed to the surface of the coating with an ethyl-2-cyanoacrylate based adhesive and then loaded into a Positest Adhesion tester. The dollies were then left to set. The Positest instrument then applied a uniform and increasing force to remove the dolly from the substrate, and the load is increased at a steady rate until the coating fails or the substrate breaks. A stand-off is used to keep the substrate still while the pull-off force is applied. A schematic diagram of the Positest is shown in Figure 5.

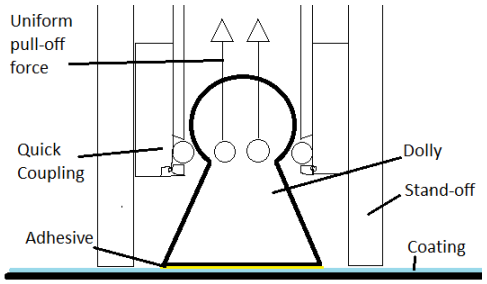

Figure 5: A schematic diagram of a dolly fixed to the coating surface, the dolly, stand-off, coupling, and uniform pull-off force lines are all labelled.

Pull tests performed on the ARC were carried out using a dolly size of 20mm, with the standard ethyl-2-cyanoacrylate based adhesive. The dollies were sanded with 120 grit sandpaper and were glued 6 days prior to testing. The dollies were pulled at a rate of 0.7MPa/s. The coating withstood a maximum load of 4.92MPa before the glass substrate failed. Figure 6 shows the glass substrate cracked and still partially stuck to the dolly (~45%). The glue is on the remaining surface of the dolly, and was removed from the surface of the coating. The coating was still intact across the entire surface of the glass—providing evidence that the sol-gel ARC has good adhesion.

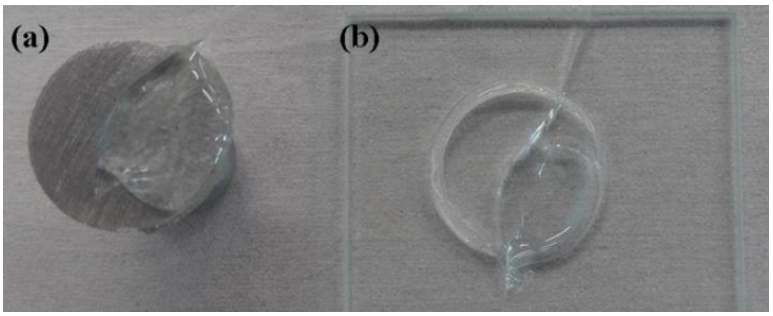

Figure 6: (a) The base of a dolly with glass adhered to the surface, revealing no coating delamination. (b) A fractured sample of the ARC on glass after a pull test. The coating remained undamaged. Image courtesy of TWI.

4.1.2 Cross-Hatch Test

In the standard test, a pattern consisting of 6 parallel lines is created by scratching the coating using a round, 6-bladed, steel cutting knife manufactured by Dyne Technology Inc. (model number: CC1000). Then, 6 parallel lines are scratched, intercepting the initial lines at 90° to create a cross-hatch pattern. The ARC displayed no visible damage after the cross-hatch test. The ARC therefore has a score of 0 according to ISO 9211-4 (ISO 2012), indicating excellent adhesion.

4.2 High temperature stability

The ARC has a complex structure with internal bubbles. ARC samples were heated at 100°C intervals up to 600°C. Before heat treatment, the surface of the ARC is featureless. After heat treatment, the optical properties of the coating are affected. Figure 7 (a) shows that

damage begins to occur in the coating at above 100°C heat treatment, and Figure 7 (b) shows severe damage is established at 200°C.

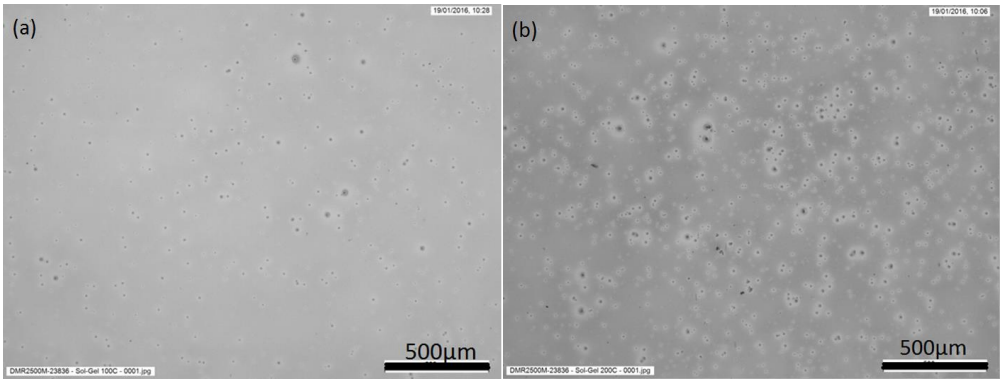

Figure 7: (a) The surface of an ARC sample after heat treatment at 100°C for 30min. (b) The surface of an ARC sample after heat treatment at 200°C for 30min, showing greater numbers of speckled features. Image courtesy of TWI.

Across the 350nm to 850nm wavelength range, the WAR of the samples had decreased from 2.6% to 2.28% after exposure to 400°C, and 2.02% after exposure to 500°C. In Figure 8 in can be seen that bubbles are formed within the ARC after exposure to 700°C causing the appearance of blurry circles on the ARC surface. The WAR of the sample had increased to 3.2%.

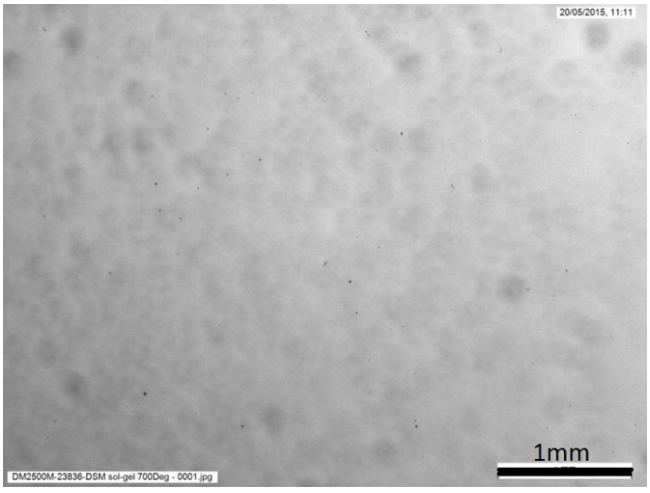

Figure 8: The surface of an ARC sample after exposure to 700°C for 30min, blurry circles indicate the formation of larger voids beneath the coating surface.

4.3 Resistance to temperature and humidity

In accordance with IEC 61646, 2 samples of the ARC were loaded into an environmental chamber (Sanyo Gallenkamp HCC065) and held at 85°C and 85% relative humidity (RH) for a total of 1000 hours. The reflectance of the samples was measured using a spectrophotometer at the beginning, on completion of the 1000 hour test, and also at the mid-way point (500 hours). Table 2 shows the effect of damp heat (DH) exposure on the reflectance of two ARC samples. Before each measurement the samples were cleaned in a 50-50 IPA and DI water mix, to isolate the effect of the DH test.

Table 2: Measured WAR of ARC samples after DH exposure:

	Sample 1	Sample 2
Initial	2.25%	2.35%
500 hours	2.25%	2.23%
1000 hours	3.19%	2.85%

After 500 hours, the change in WAR was negligible. A slight reduction in WAR in sample 2 is most likely caused by a change in coating porosity percentage or the coating thinning after prolonged heat exposure. After 1000 hours, the WAR of the samples 1 and 2 had increased by 0.94% and 0.62% respectively. The WAR of samples 1 and 2 had increased by 0.94% and 0.62% respectively, indicating the coating is susceptible to damage from hot and humid environments. The surfaces of the samples appeared to have been affected by water exposure from the DH test. After 1000 hours, water marks are clearly visible as shown in Figure 9.

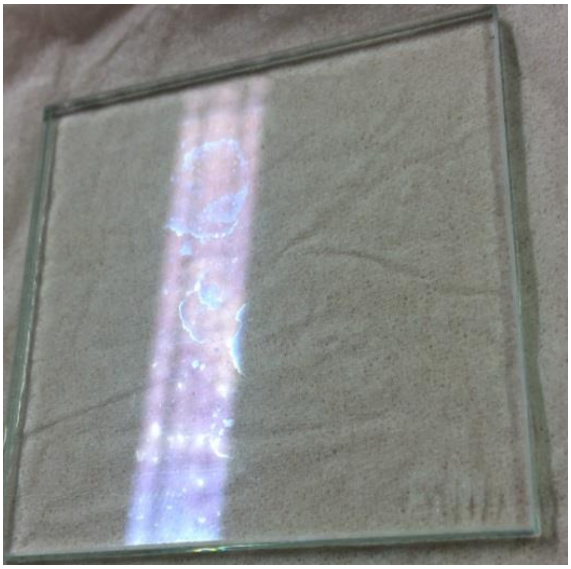

Figure 9: Optical image of sample 1 showing signs of water damage after 1000hrs of DH exposure. Image courtesy of TWI.

4.4 Water contact angle

The water contact angle of the ARC was measured to be 9° with a Kruss surface energy analyser (DSA100). A water contact angle of 9° means the coating is hydrophilic. The coating appears to absorb water. This is a concern for the long term performance of the ARC: if the coating absorbs water, the optical properties are diminished as the presence of water raises the refractive index of the coating. However, measuring this effect is difficult as the majority of water evaporates before and during reflectance measurements. A water contact angle measurement on the surface of an ARC sample is shown in Figure 10.

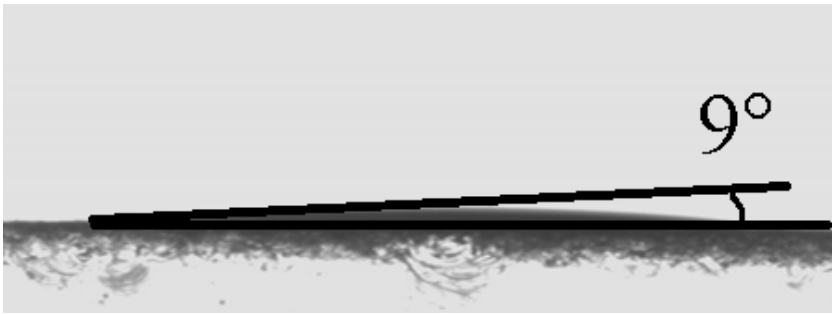

Figure 10: A water drop on the surface of the ARC with a contact angle of 9°. Image courtesy of TWI.

4.5 Stability against thermal cycling

Samples of the ARC were exposed to thermal cycling in accordance with IEC 61646. The samples were loaded into a Vötschtechnik VCS 7430-4 environmental chamber and cycled

between -40ºC and 85ºC, with a minimum dwell time of 10 minutes at each temperature. As shown in Figure 11, thermal cycling had a positive effect on the WAR of the samples, indicating the samples are resistant to thermal damage. However, the change in WAR suggests the ARC is no longer as it was deposited and therefore the mechanical properties of the ARC may have been compromised. This result agrees with the resistance to remarkably high temperatures demonstrated in section 4.2.

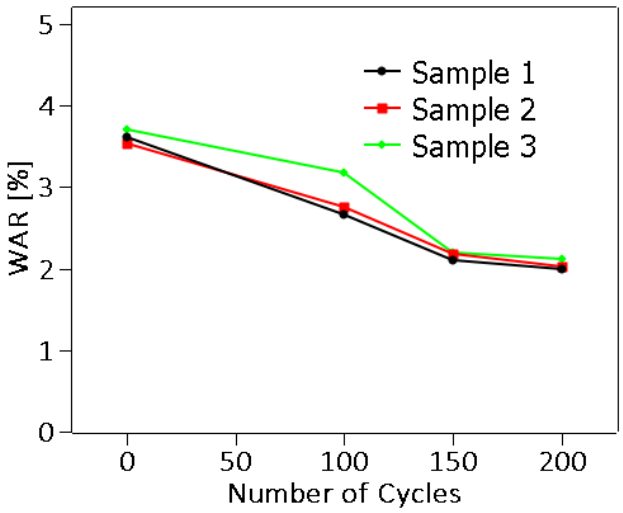

Figure 11: The measured WAR of ARC samples cycled 0, 100, 150, and 200 times between -40ºC and 85ºC in a climatic chamber (~33Hrs).

Considering the WAR before and after the test, it can be concluded that the effect of thermal cycling was a reduction in sample WAR.

4.6 Water Solubility Test

ARC samples were exposed to solubility tests sequentially in accordance with ISO 9211-4(ISO 2012). The least aggressive test is the immersion of the samples into DI water for up to 96 hours. After immersion, the samples were dried and the reflectance of the sample was measured. Initially the WAR of the ARC samples was reduced, suggesting a change in the coating structure. After the initial reduction with further exposure WAR increased, as shown in Figure 12. An increase in WAR was measured after 24 hours immersion and WAR continues to increase as the exposure time increases up to 96 hours. The WAR of the sample was measured after 6, 24, and 96 hours.

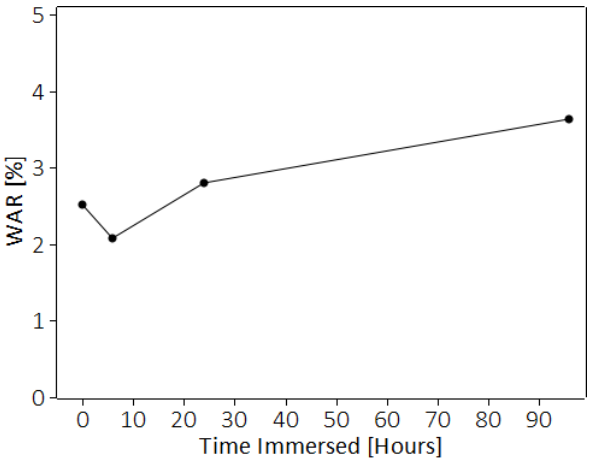

Figure 12: The WAR of ARC samples after immersion in DI water for 0, 6, 24, and 96Hrs.

The samples were then placed in boiling DI water for 5, 10, and 15 minute periods. No physical degradation was observed after 15 minutes. The WAR of the sample decreased after exposure to boiling water, as shown in Figure 13. This is consistent with heat having a positive effect on coating thickness uniformity. The results shown in Figure 12 suggest damage from water occurs on a timescale of hours.

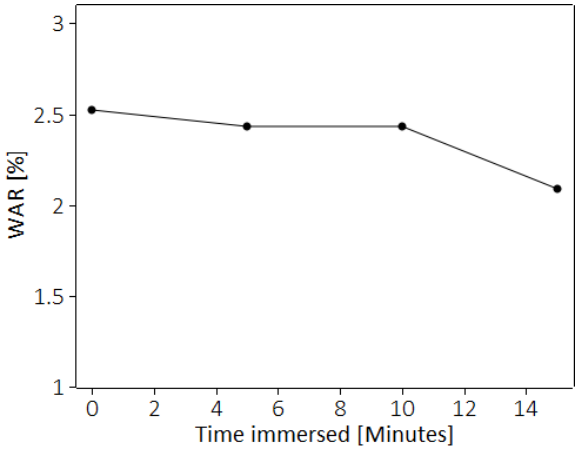

Figure 13: The WAR of ARC samples after immersion in boiling DI water for 0, 5, 10 and 15mins.

In accordance with the final test in ISO 9211-4, the samples were placed in boiling DI water for 2 minutes and then immersed in room temperature DI water for 1 minute. This process was repeated 10 times and WAR measurements were taken after the 1st, 2nd, 5th, and 10th cycle. The samples displayed no visible degradation. The WAR was decreased after the first 2 cycles then remained relatively constant. The WAR of the samples is shown in Figure 14.

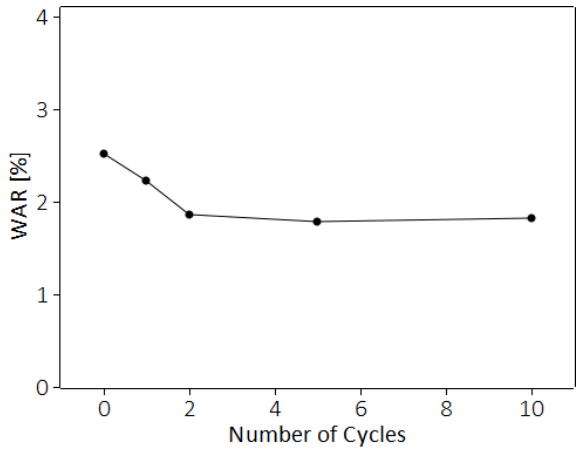

Figure 14: The WAR of samples of ARC after 0, 1, 2, 5, and 10 cycles of 2 minutes in boiling DI water, followed by 1 minute in room temperature DI water.

4.7 Abrasion Resistance

A felt pad abrasion test from BS EN 1096-2 (BSI 2002) ,which uses a slow turning circular abrader, was adapted into a linear abrasion test. In the adapted test, a felt abrader with a surface area of ~7.5mm^2 was applied to the surface of the ARC coating with a force of 10N. It was then passed across the surface 100 times, with a stroke length of 30mm and a speed of 60 cycles per minute. This increased the WAR of the sample relatively by 33% from 2.75% to 3.65%.

The CS-10(ASTM 2013) abrader was pressed to the surface of ARC samples with a force of 5N and 10N. The abrader was then repeatedly passed over the sample surface at 60 cycles per minute with a stroke length of 30mm. After 100 cycles at each force, the coatings were cleaned in an ultrasonic bath and the WAR was measured. This resulted in an absolute increase in WAR of 1.32% and 2.21% for 5N and 10N respectively. The increase in WAR is due to severe damage to the coating. This result suggests wear and tear is an issue for sol-gel ARCs.

4.8 Acid Attack

As acid rain is common in many cities around the world, it is important to test the acid resistance of any commercial sol-gel coating. ARC samples were submerged in dilute sulfuric acid (BSI 2002) with a pH of ~3.5. The type of acid and pH were selected to simulate acid rainwater(ASTM 2006). The pH of the solution was measured using an Accumet AB150 pH meter. The WAR of the coating was measured after every 30 minutes of exposure. Figure 15 shows the resulting WAR of the samples after exposure to acid for lengths of time.

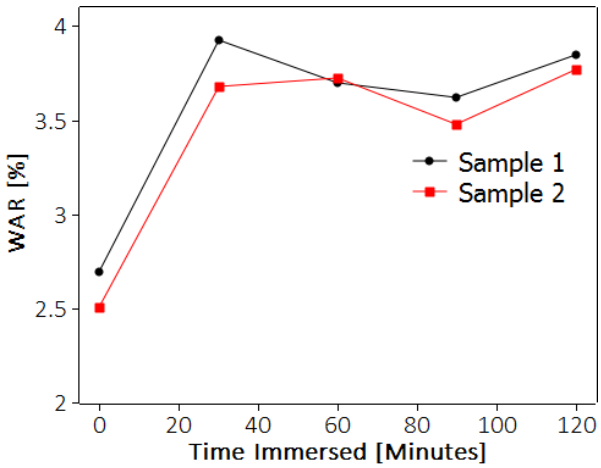

Figure 15: The WAR of sol-gel samples after exposure to dilute sulphuric acid, simulating the effect of acid rain for 0, 30, 60, 90, and 120mins.

Figure 15 shows that exposure to acid over 30 minutes increases the WAR of the ARC by ~1.2%. This implies the coatings are vulnerable to acid attack.

4.9 Scratch resistance

Micro-indentation was used to measure the scratch resistance of the ARC (Kim et al. 2014). A round end cone micro-indenter with a tip radius of 5µm was used. The micro-indenter was held at a force of 0.1mN at the surface of the sample, and then the load was increased at a rate of 1mN per 1µm as the micro-indenter travelled across the surface. The micro-indenter travelled 400µm and applied a maximum force of 400mN over the 5µm micro-indenter tip, ~5kPa pressure.

An image of the resulting scratch from the micro-scratch test is shown in Figure 16. The resting pressure of 0.1mN deformed the coating at ~30nm. Figure 16 shows debris begins to appear next to the scratch very early, implying partial delamination at ~20-40mN. This point on the scratch is indicated in Figure 16, labelled ‘Delamination initiates’. At ~180-200mN, it appears the debris from the coating is much larger and shows interference effects, indicating the coating has begun to delaminate completely. In Figure 17, this point is indicated by the label reading ‘Total delamination occurs’. There are no cracks extending from the scratch, implying the coating is structurally sound.

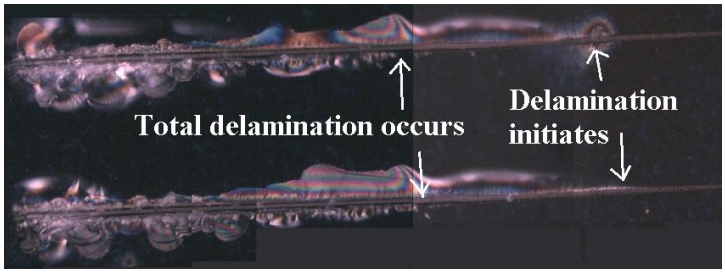

Figure 16: Scratches in the surface of an ARC sample. The scratches were produced by pressing a micro-indenter into the surface of the coating and moving the sample as the load is increased. Image courtesy of TWI.

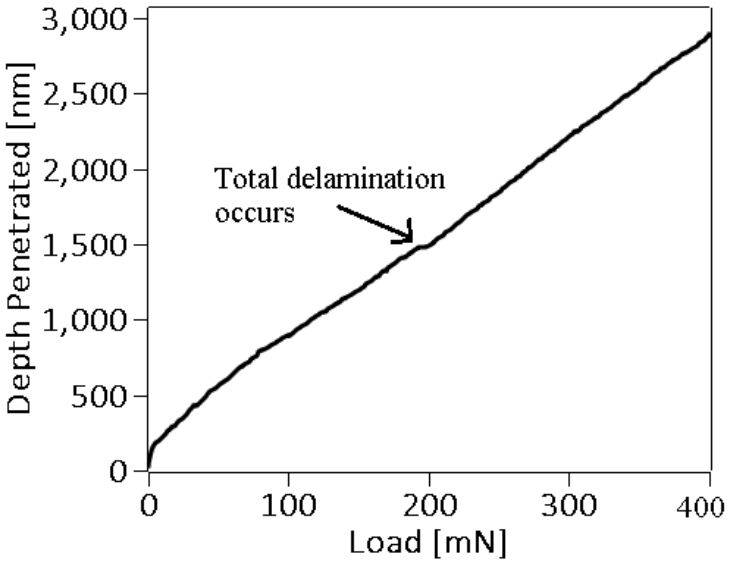

Figure 17: Plot of the load applied to the micro-indenter against depth penetrated into the surface of the ARC sample.

5 Discussion

Solar modules are installed with a typical 25 year warranty. It is important that the adhesion and durability of a coating applied to solar modules is consistent with the warranty offered with solar modules. The coating is expected to withstand humidity, temperature cycles, and acid rain. The coating must also be scratch resistant to prevent damage during maintenance. The performance of a commercially sourced, single-layer, sol-gel ARC was evaluated. The coating proved to be an optically effective AR, resulting in a 69-74% reduction in reflection losses when a weighted average was taken across varying wavelengths. Considering the cost and ease of application of simple porous silica coatings, this is an impressive reduction in reflection losses.

The adhesion of the ARC has been tested using standard test methods. The pull test (ISO 4624) did not remove the ARC from the substrate. The highest recorded pull strength that failed to delaminate the coating was 4.92MPa. The substrate shattered in every pull test and the coating was intact. After the samples had undergone the cross-hatch test (ISO 9211-4), minimal delamination from the application and removal of tape was observed. In addition to these standard test methods, a micro-indentation scratch test was used, demonstrating the excellent scratch resistance of the ARC. Therefore, the sol-gel ARCs are mechanically strong and durable.

Pre-coating solar glass is very desirable for cover glass applications on thin film CdTe modules. The CdTe PV manufacturing process involves temperatures as high as 500°C. Any solar panel coating designed for use on CdTe needs to withstand comparable temperatures. This study has shown the sol-gel ARC is heat resistant and begins to bubble and deform at temperatures greater than those used in the CdTe absorber deposition and activation processes. Although visual degradation is seen after heat treatment at 100°C, heat treatment of the ARC did not increase the WAR until heat treatment temperatures exceeded 500°C. The optical properties are affected only beyond heat treatment of 700°C, when bubbles within the coating appeared to form. This means the coatings are stable beyond temperatures that would affect the cover glass.

The acid attack test simulates the pH of acid rain. However, the exact chemical character of acid rain differs outside of the laboratory. An updated acidic test should be developed for coatings likely to be exposed to acidic conditions. The updated test should use more representative liquids to better simulate rain water. Damp heat and acid attack tests resulted in an increase in the reflectance of the ARC. In contrast, thermal cycling and exposure to boiling water reduced the WAR of the ARC. Thermal treatment of the ARC improved transmission, suggesting the ARC benefits from curing. In future work, mechanical tests performed before and after heat treatment would establish whether the mechanical strength of the coating has been affected. The ARC is vulnerable to water ingress and has a very low water contact angle. The combination of tests presented in this work demonstrates that sol-gel coatings are damage resistant. However, long term exposure to water and/or acid damages the ARC. Additionally the effectiveness of the ARC was reduced after abrasion tests. A fully closed surface, impenetrable by water, is imperative in future sol-gel coatings. Vulnerability to acid attack and damp heat limits the ability of single-layer sol-gel derived ARCs to meet

the industry standard of 25 years in the field, particularly in the presence of acidic rain, sand or grit, or in tropical climates.

While the aim of this work is to test the durability and effectiveness of a commercially available sol-gel ARC, it is important to stress that that there is a great variety of sol-gel coatings and that continuous progress is being made in the field. The present study on one type of sol-gel coating provides an interesting insight into their performance and durability. However, it would be dangerous to make generalised conclusions until a wider range of formulations have been tested.

6 References

A. E. Conrady, 1929. *Applied Optics and Optical Design Part One*, Oxford UK: Oxford University Press.

Arfsten, N.J., Habets, R.A.D.M. & Buskens, P.J.P., 2011. Inorganic oxide coating.

ASTM, 2006. Standard Test Method for Accelerated Acid Etch Weathering of Automotive Clearcoats Using a Xenon-Arc Exposure Device. *ASTM D7356/D735*.

ASTM, 2002. Standard Test Method for Pull-Off Strength of Coatings Using Portable Adhesion Testers. *ASTM D4541*.

ASTM, 2013. Standard Test Method for Resistance of Transparent Plastics to Surface Abrasion. *ASTM D1044-13*.

Brinker, C.J. & Scherer, G.W., 1990. *Sol-Gel Sciencea*, New York: Academic Press.

BSI, 2002. Glass in building. Coated glass. Requirements and test methods for class A, B and S coatings. *Bs En 1096-2:2012*.

Buskens, P. et al., 2016. Antireflective Coatings for Glass and Transparent Polymers. *Langmuir*, 32(27), pp.6781–6793.

Cai, S. et al., 2014. Sol-gel preparation of hydrophobic silica antireflective coatings with low refractive index by base/acid two-step catalysis. *ACS Applied Materials and Interfaces*, 6(14), pp.11470–11475.

Çamurlu, H. et al., 2012. Sol-gel thin films with anti-reflective and self-cleaning properties. *Chemical Papers*, 66(5), pp.461–471. Available at: http://www.degruyter.com/view/j/chempap.2012.66.issue-5/s11696-012-0144-4/s11696-012-0144-4.xml.

Chen, C.H. et al., 2011. Scratch-resistant zeolite anti-reflective coating on glass for solar applications. *Solar Energy Materials and Solar Cells*, 95(7), pp.1694–1700.

Cooper, G.I. & Cox, G. a., 1996. The aqueous corrosion of potash-lime-silica glass in the range 10-250??C. *Applied Geochemistry*, 11(4), pp.511–521.

Deubener, J. et al., 2009. Glasses for solar energy conversion systems. *Journal of the European Ceramic Society*, 29(7), pp.1203–1210.

Fabes, B.., Zelinski, B.J.J. & Uhlmann, D.R., 1993. Sol-Gel Derived Ceramic Coatings. In J. B. Wachtman & R. A. Haber, eds. *Ceramic Films and Coatings*. Park Ridge: Noyes, pp. 224–284.

Faustini, M. et al., 2010. Preparation of Sol - Gel Films by Dip-Coating in Extreme Conditions. *Journal of Physical Chemistry C*, 114(17), pp.7637–7645. Available at: http://pubs.acs.org/doi/abs/10.1021/jp9114755.

Guo, Z. et al., 2006. Surface functionalized alumina nanoparticle filled polymeric nanocomposites with enhanced mechanical properties. *Journal of Materials Chemistry*, 16(27), p.2800. Available at: http://xlink.rsc.org/?DOI=b603020c.

Guo, Z.Q. et al., 2017. Super-durable closed-surface antireflection thin film by silica nanocomposites. *Solar Energy Materials and Solar Cells*, 170(November 2016), pp.143–148.

Han, Y.-H. et al., 2007. Sol–gel-derived organic–inorganic hybrid materials. *Journal of Non-Crystalline Solids*, 353(3), pp.313–320. Available at: http://linkinghub.elsevier.com/retrieve/pii/S0022309306006478.

IEC, 2016. IEC 61215-1:2016.

ISO, 2012. Optics and photonics - Optical coatings, Part 4: Specific test methods. *ISO 9211-4*.

ISO, 2002. Paints and varnishes -- Pull-off test for adhesion. *ISO 4624*.

Kaminski, P.M., Lisco, F. & Walls, J.M., 2014. Multilayer Broadband Antireflective Coatings for More Efficient Thin Film CdTe Solar Cells. *IEEE Journal of Photovoltaics*, 4(1), pp.452–456.

Kim, R.H. et al., 2014. Non-volatile organic memory with sub-millimetre bending radius. *Nature Communications*, 5(3583).

Mammeri, F. et al., 2005. Mechanical properties of hybrid organic-inorganic materials. *J. Mater. Chem.*, 15(35-36), pp.3787–3811. Available at: http://dx.doi.org/10.1039/B507309J.

Meredith, P. & Harvey, M., 2006. Silica and silica-like films and method of production. , pp.1–15.

Osterwald, C.R. & McMahon, T.J., 2008. History of Accelerated and Wualification Testing of Terrestrial Photovoltaic Modules: A Literature Review. *Prog. Photovolt: Res. Appl.*, 17, pp.11–33.

Pagliaro, M., Ciriminna, R. & Palmisano, G., 2009. Silica-based hybrid coatings. *Journal of Materials Chemistry*, 19(20), p.3116.

Sanchez, C. et al., 2011. Applications of advanced hybrid organic–inorganic nanomaterials: from laboratory to market. *Chem. Soc. Rev.*, 40(2), pp.696–753.

Schottner, G., 2001. Hybrid Sol - Gel-Derived Polymers : Applications of Multifunctional Materials. *Chem.Mater*, 13, pp.3422–3435.

Tao, C. et al., 2016. Sol-gel based antireflective coatings with superhydrophobicity and exceptionally low refractive indices built from trimethylsilanized hollow silica nanoparticles. *Colloids and Surfaces A: Physicochemical and Engineering Aspects*, 509, pp.307–313.

Thies, J.C. et al., 2011. Method of preparing nano-structured surface coatings and coated articles. , pp.1–24.

Vicente, G.S., Bayón, R. & Morales, A., 2008. Effect of Additives on the Durability and Properties of Antireflective Films for Solar Glass Covers. *Journal of Solar Energy Engineering*, 130(1), p.011007.

Vilarigues, M. & da Silva, R.C., 2006. Characterization of potash-glass corrosion in aqueous solution by ion beam and IR spectroscopy. *Journal of Non-Crystalline Solids*, 352(50-51), pp.5368–5375.

Wang, N. & Xiong, D., 2014. Comparison of micro-/nano-hierarchical and nano-scale roughness of silica membranes in terms of wetting behavior and transparency. *Colloids and Surfaces A: Physicochemical and Engineering Aspects*, 446, pp.8–14. Available at: http://dx.doi.org/10.1016/j.colsurfa.2014.01.029.

Wang, X. & Shen, J., 2010. Sol-gel derived durable antireflective coating for solar glass. *Journal of Sol-Gel Science and Technology*, 53(2), pp.322–327.

Wojdyła, A. et al., 2017. New assessment criteria for durability evaluation of highly repellent surfaces. *Wear*, 390-391(May), pp.49–60.

Womack, G. et al., 2017. Performance and durability of broadband antireflection coatings for thin film CdTe solar cells. *Journal of Vacuum Science & Technology A: Vacuum, Surfaces, and Films*, 35(2), p.021201. Available at: http://avs.scitation.org/doi/10.1116/1.4973909.

Womack, G., Kaminski, P.M. & Walls, J.M., 2015. High temperature stability of broadband Anti-Reflection coatings on soda lime glass for solar modules. *2015 IEEE 42nd Photovoltaic Specialist Conference, PVSC 2015*, pp.1–3.

Xu, J. et al., 2017. Superhydrophobic silica antireflective coatings with high transmittance via one-step sol-gel process. *Thin Solid Films*, 631, pp.193–199. Available at: http://dx.doi.org/10.1016/j.tsf.2017.03.005.